The Journal of Chemical Physics

RESEARCH ARTICLE | JUNE 26 2023

Effect of external electric fields in the charge transfer rates of donor–acceptor dyads: A straightforward computational evaluation

Pau Besalú-Sala ; Alexander A. Voityuk ; Josep M. Luis ; Miquel Solà

J. Chem. Phys. 158, 244111 (2023)
https://doi.org/10.1063/5.0148941

AIP Publishing

The Journal of Chemical Physics ARTICLE pubs.aip.org/aip/jcp

Effect of external electric fields in the charge transfer rates of donor–acceptor dyads: A straightforward computational evaluation

Cite as: J. Chem. Phys. 158, 244111 (2023); doi: 10.1063/5.0148941
Submitted: 3 March 2023 • Accepted: 5 June 2023 •
Published Online: 26 June 2023

Pau Besalú-Sala, Alexander A. Voityuk, Josep M. Luis,[a] and Miquel Solà[a]

AFFILIATIONS

Institut de Química Computacional i Catàlisi and Departament de Química, Universitat de Girona, E-17003 Girona, Catalonia, Spain

[a]Authors to whom correspondence should be addressed: josepm.luis@udg.edu and miquel.sola@udg.edu

ABSTRACT

We present a straightforward and low-cost computational protocol to estimate the variation of the charge transfer rate constant, k_{CT}, in a molecular donor–acceptor caused by an external electric field. The proposed protocol also allows for determining the strength and direction of the field that maximize the k_{CT}. The application of this external electric field results in up to a >4000-fold increase in the k_{CT} for one of the systems studied. Our method allows the identification of field-induced charge-transfer processes that would not occur without the perturbation caused by an external electric field. In addition, the proposed protocol can be used to predict the effect on the k_{CT} due to the presence of charged functional groups, which may allow for the rational design of more efficient donor–acceptor dyads.

INTRODUCTION

Charge transfer (CT), also known as electron transfer (ET) reactions, is ubiquitous in biology and chemistry. In biology,[1] ET reactions can be found, for instance, in redox enzymes[2,3] or in the activation of sensory proteins,[4] but also in fundamental processes such as nerve impulse transmission,[5] photosynthesis,[6] cellular respiration,[7] or DNA UV-damage repair,[8] among others. In chemistry, there are many reactions that can be classified as ET reactions. The most obvious example is constituted by the group of oxidation-reduction reactions.[9] Other examples include the proton-coupled electron transfer (PCET) reactions[4] as well as all reactions carried out under photocatalytic conditions.[10,11]

Charge transfer reactions are also in the core of organic solar cells (OSCs). Solar cells are needed to harvest solar energy and convert it into electricity, reducing the use of coal and oil. Such a transition toward competitive low carbon-fingerprint energy harvesting technologies is the seventh goal of the United Nations Sustainable Development Agenda for 2030 and UNESCO's World Heritage.[12] OSCs represent a promising alternative to building photovoltaic devices owing to their easier manufacturing, lower weight, flexibility, and associated cost.[13–15] When designing OSCs constructed using the molecular heterojunctions (MHJs)[16] approach, the electron acceptor and electron donor are covalently linked, forming a donor–acceptor (D–A) dyad. Compared to OSCs based on bulk heterojunction structures, MHJs allow better structural control and charge mobility tuning, which are notable advantages for the difficult task of optimizing the performance of charge separation processes. Although these MHJ organic cells are not implemented in real organic cells, the studied dyads can be used as model systems to understand the photoinduced electron transfer processes that occur in OSCs.

Computational modeling can help improve the design of D–A dyads with high charge-transfer rate constants.[17–20] In this work, we present a computationally inexpensive protocol to determine the effect of the oriented external electric fields (OEEFs) on the rate of the charge transfer process, k_{CT}. Our methodology can be used to speed up *any* charge transfer process by applying an OEEF, although, in this work, we decided to focus our study on the changes in k_{CT} induced by an OEEF in the case of four fullerene-based dyads (Fig. 1): *trans*-2 C_{60}-ZnTPP (**ZnTPP**),[21] C_{60}-triphenylamine (**TPA**),[22,23] C_{60}-3,6-di^{t}Bu-Azulene (**Az**),[24] and C_{59}N-phthalocyanine (**PC**).[25]

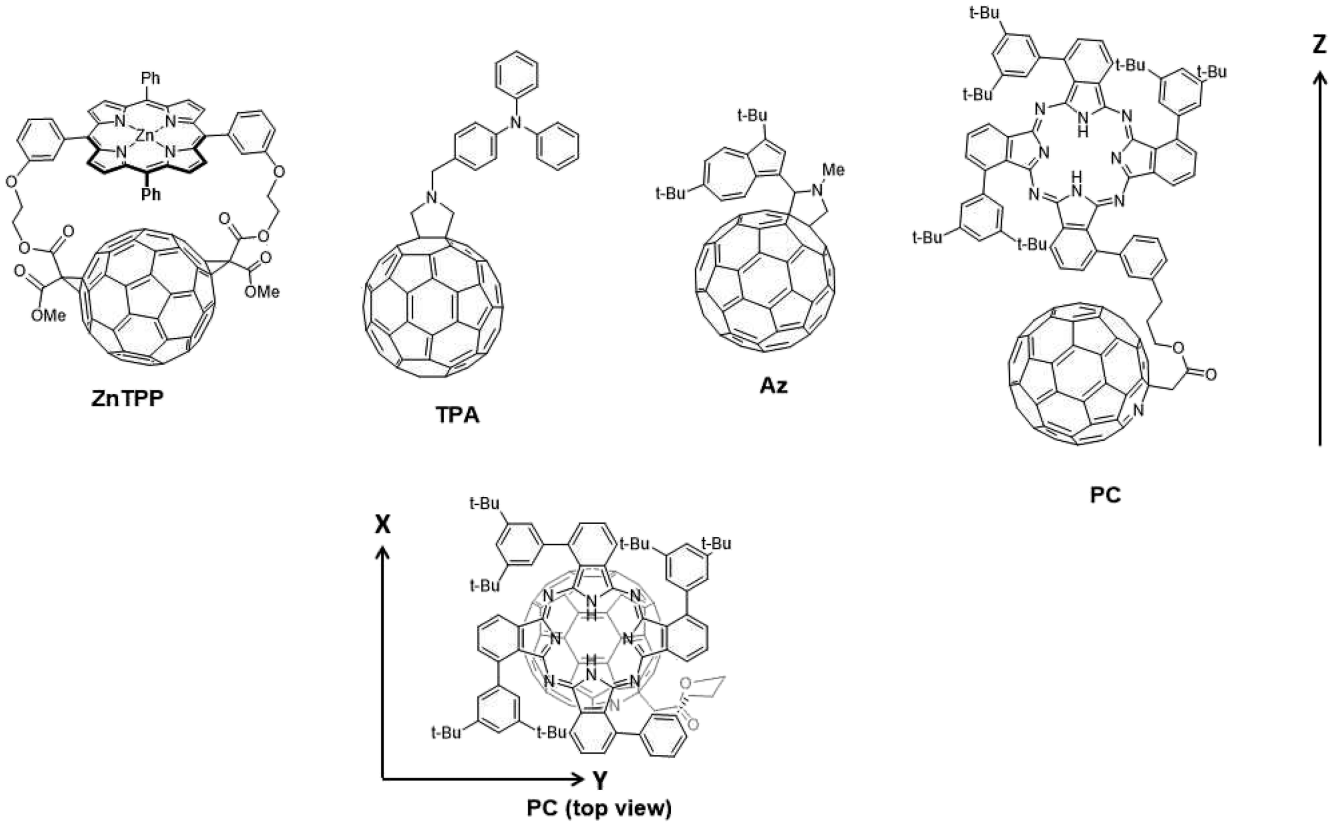

FIG. 1. The donor–acceptor dyads studied in this work and their orientation in the Cartesian space.

Within Marcus theory,[26–28] the charge transfer rate depends exponentially on the negative of the square of the sum of the reorganization energy, λ, and the Gibbs energy change in the electron transfer process, ΔG,

$$k_{CT} = \frac{2\pi}{\hbar} V_{DA}^2 \frac{1}{\sqrt{4\pi\lambda k_B T}} \exp\left(-\frac{(\lambda + \Delta G)^2}{4\lambda k_b T}\right), \tag{1}$$

where $\hbar$ refers to the reduced Planck constant and k_B to the Boltzmann constant. In most D–A dyads, the excitation is delocalized over D and A and oscillates back and forth between them to finally populate the most stable local excited state [LES_1, $(D–A)^*$],[29] which can be located on D or A or delocalized among D and A. The charge transfer preferably occurs in the transition from LES_1 to the most stable charge transfer state (CTS_1, $D^+–A^-$).[30–32] Therefore, the ΔG to be estimated in Eq. (1) is $\Delta G = \Delta G_{LES1\rightarrow CTS1} = \Delta G_{CTS1} - \Delta G_{LES1}$, where ΔG_i is the Gibbs energy difference between the *i*th excited state and the ground state. A good D–A dyad must show fast charge separation (i.e., high k_{CT}) and slow charge recombination. Here, we investigate how OEEF can be used to increase the k_{CT} in D–A dyads. When the D–A dyads present a random orientation in space, an OEEF cannot be directly applied to improve the efficiency of their charge transfer process. However, once the direction and strength of the most suitable electric field for optimizing the charge-transfer process for a given dyad are determined, it is possible to redesign the dyad by placing charged or polar functional groups at certain positions to locally generate the required electric field and, therefore, increase the efficiency of the charge transfer process.

According to Eq. (1), the maximum value of the rate constant is observed when ΔG = −λ. This constraint can be imposed by modifying ΔG, λ, or both with an external perturbation, such as an OEEF. Despite the fact that the effect of internal or local EF has been acknowledged,[33] measurements of charge transfer rates in D–A dyads under OEEFs are very scarce.[34–36] In order to identify the optimal OEEF to speed up a charge transfer process, it would be ideal to develop an inexpensive computational tool to predict the impact of the OEEF on k_{CT}.

The study of the effect of OEEF on reactivity is a hot topic nowadays.[37–44] In a previous study, some of us reported a method to predict the effect of an OEEF on the rate and selectivity of a chemical reaction based on the Taylor expansion of the field-dependent energy of the reactants and transition states in terms of their field-free dipole moments and electrical (hyper)polarizabilities.[45] Here, we propose to use an equivalent approach to evaluate the changes induced by an OEEF in the relative energy of the excited states of a molecule. The field-dependent relative Gibbs energy of the *i*th excited state, $\Delta G_i(\mathbf{F})$, is given by

$$\Delta G_i(\mathbf{F}) = \Delta G_i(0) - \Delta\mu_i\mathbf{F} - \Delta\alpha_i\mathbf{F}^2 + O(\mathbf{F}^3), \quad (2)$$

where $\Delta G_i(0)$, $\Delta\mu_i$, and $\Delta\alpha_i$ correspond, respectively, to the field-free relative Gibbs energy of the *i*th excited state and the differences between the electronic dipole moment and electronic polarizability of the *i*th excited state and the ground state. Equation (2) allows the estimation of the change in the relative Gibbs energy of the excited states due to the presence of an arbitrary OEEF only from data obtained in field-free calculations and, therefore, without the need to perform calculations including the OEEF explicitly.

For practical use, Eq. (2) must be truncated at a point that balances the desired accuracy and the computational cost. In a previous study, some of us showed that the truncation of the Taylor expansion of the field-dependent energy at the quadratic (i.e., polarizability) term accurately predicts the changes in the rate and the selectivity of a chemical reaction at a very low computational cost.[45] Here, we have used Eq. (2) to predict the field-dependent Gibbs energies of the excited states of the photoactive systems **ZnTTP**, **TPA**, **Az**, and **PC** and, subsequently, determine the optimal OEEF that maximizes their k_{CT} by imposing the constraint $\Delta G = -\lambda$. For **ZnTTP**, we have also compared the k_{CT} obtained from Eq. (2) with corrections up to the second order with the one obtained by means of explicit OEEF calculations as a benchmark of the accuracy of the presented method.

As for many D–A dyads, the first and second excited states of **ZnTTP** correspond to the most stable charge transfer state (CTS_1) and the most stable local excited state (LES_1), respectively. Specifically, the electron-transfer $LES_1 \rightarrow CTS_1$ can be conceptualized as the movement of one electron from the porphyrinic ring (the donor unit) to the C_{60} (the acceptor unit). Interestingly, a judiciously applied OEEF enhances the k_{CT} value (*vide infra*), while the charge recombination process is expected to be slowed down as the OEEF pulls the electron density away from the generated hole. Once the methodology was validated for **ZnTTP**, it was also applied to the other systems under study, namely **TPA**, **Az**, and **PC**. We finalize our work by studying the k_{CT} of **ZnTTP** with the point-charges located in space to generate an OEEF similar to the optimal OEEF determined with our new methodology. We show that in this point-charge model, the k_{CT} is enhanced, thus paving the path toward the design of more efficient dyads.

METHODOLOGICAL DETAILS

We have obtained the ground-state equilibrium geometry at the B3LYP-D3(BJ)/6-311G(d,p) level of theory[46–50] for each structure from somewhere else.[51] The donor and acceptor geometries needed to estimate the internal reorganization energy were obtained at the same level of theory as the ground state equilibrium geometries.

Twenty to one hundred lowest-lying singlet excited states for each D–A pair were computed using the time-dependent density functional theory (TDDFT) formalism[52–58] at the CAM-B3LYP level of theory expanding the orbitals with the double-ζ with polarization Def2SVP[59] basis set at the ground-state equilibrium geometry. As several works[60–63] prove, except for a few cases,[64] changes in k_{CT} are minor if one considers the effect of the geometrical relaxation in the LES_1. Indeed, in the case of fullerenes, the change in the equilibrium geometry in the transition from the ground state to the LES_1 is minor, as can be seen from the root mean square deviation, RMSD, values given in Table S5 of the supplementary material. CAM-B3LYP[65] has been reported to be one of the best density functional approximations for the evaluation of CTS.[51] Both the ground and excited state calculations were performed with the Gaussian16 package.[66]

Nature of the excited states

A quantitative analysis of exciton delocalization and charge separation is carried out in terms of the transition density matrix $\mathbf{T^{0i}}$ of the *i*th excited state (Φ_i^*). This analysis is performed on the more convenient Löwdin orthogonal basis. The matrix ${}^{\lambda}\mathbf{C}$ of the molecular orbital (MO) coefficients expanded in a basis of orthogonalized atomic orbitals is obtained from the coefficients $\mathbf{C}$ in the original atomic basis ${}^{\lambda}\mathbf{C} = \mathbf{S}^{1/2}\mathbf{C}$, where $\mathbf{S}$ is the atomic orbital overlap matrix. The transition density matrix $\mathbf{T^{0i}}$ for an excited state Φ_i^* is constructed as a superposition of singly excited configurations[67,68] where an occupied MO ψ_j in the ground state is replaced by a virtual MO ψ_a and is computed as

$$T^{0i}_{\alpha\beta} = \sum_{ja} A^{i}_{j\rightarrow a}\, {}^{\lambda}C_{\alpha j}\, {}^{\lambda}C_{\beta a}, \quad (3)$$

where $A^{i}_{j\rightarrow a}$ are the expansion coefficients corresponding to the ith excited state and alpha and beta are atomic orbitals.

The excitation weight $\Omega^i(D, A)$ is determined by

$$\Omega^i(D,A) = 1/2 \sum_{\alpha\in D,\ \beta\in A} \left(T^{0i}_{\alpha\beta}\right)^2. \quad (4)$$

The weights of local excitations on D and A are $\Omega^i(D, D)$ and $\Omega^i(A, A)$, respectively. The weight of electron transfer configurations D → A and A → D is represented by $\Omega^i(D, A)$ and $\Omega^i(A, D)$. Therefore, the quantity $CS^i = \Omega^i(D, A) - \Omega^i(A, D)$ describes charge separation between D and A, and the $CT^i = \Omega^i(D, A) + \Omega^i(A, D)$ is the total weight of CT configurations in the excited state Φ_i^*. With this methodology, CT states (CTS) and local excited states (LES) can be easily identified. In LES, the excitation is mostly localized on a single fragment (CS < 0.1 e), whereas in CTS, the electron density is transferred between D and A (CS > 0.9 e).

Electronic coupling

We used the Fragment Charge Difference (FCD) method to derive the coupling of LES and CTS calculated with TDDFT.[69] Within the two-state model, the D–A coupling is given by

$$V_{DA} = \frac{(E_i - E_j)|\Delta q_{ij}|}{\sqrt{(\Delta q_i - \Delta q_j)^2 + 4(\Delta q_{ij})^2}}, \quad (5)$$

where Δq_i and Δq_j are the difference in the donor and acceptor charges in the adiabatic states Φ_i and Φ_j, respectively, and Δq_{ij} is the charge difference computed from the $\Phi_i \rightarrow \Phi_j$ transition density matrix. Several years ago, the Fragment Charge Difference (FCD) method was extended to calculate the electronic couplings and diabatic energies for photoinduced reactions.[69] FCD was shown to provide consistent values of the ET parameters for two- and multi-state model systems. It was suggested how to identify situations where the two-state scheme can be applied and where it will fail

to provide satisfactory results. In our present work, we used these criteria[69] to thoroughly check whether the two-state model can be applied to derive electronic couplings.

Reorganization energy, λ

The total reorganization energy can be decomposed into the internal and external contributions (λ_{int} and λ_{ext}). λ_{int} is the average of the energy required to distort the nuclear configuration from the D^+–A^- or $(D–A)^*$ equilibrium geometry to the equilibrium geometry of the $(D–A)^*$ or D^+–A^- state without transferring an electron. λ_{ext} is the corresponding energy required to change the slow (reorientational) part of the solvent reorganization between both equilibrium geometries. In this study, λ_{int} was computed considering isolated donor and acceptor fragments, which contribute separately to the internal reorganization energy,

$$\lambda_{\text{int}} = \lambda_D + \lambda_A, \tag{6}$$

where λ_D and λ_A are the reorganization energies of the donor and acceptor, respectively. In turn, λ_D was estimated as

$$\lambda_D = \frac{1}{2}\left(\lambda'_D + \lambda''_D\right), \tag{7a}$$

$$\lambda'_D = E'_n(D) - E_n(D), \tag{7b}$$

$$\lambda''_D = E'_{ion}(D) - E_{ion}(D), \tag{7c}$$

where $E_n(D)$ and $E_{ion}(D)$ are the electronic energies of the neutral and ionic states of the donor computed at their ground-state equilibrium geometry, and $E_n'(D)$ is the energy of the neutral state computed at the equilibrium geometry of the ionic state D^+. $E_{ion}'(D)$ is the energy of D^+, estimated at the equilibrium geometry of neutral D. Similarly, we calculated λ_A using equilibrium geometries of A and A^-.

The $\lambda_{ext}(\mathbf{F})$ is difficult to estimate using polarizable continuum models of the solvent. In this work, and as a first approximation, we have not considered the dependence on the OEEF of the λ_{ext}. The reason lies in the fact that in the presence of an OEEF (especially if it is intense), the solvent molecules will be oriented in the direction of the field instead of following the electron density of the solute. In this case, nothing or little will change after a charge-transfer, and the solvent molecules will continue to be oriented in the direction of the field, i.e., a zero (or low) value for $\lambda_{ext}(\mathbf{F})$. We have calculated λ_{ext} only for the field-free calculation.

Rate constant calculation

The CT rates were computed within the nonadiabatic electron transfer theory, where the CT process $DA \rightarrow D^+A^-$ can be described by the Marcus equation [Eq. (1)]. Taking into account the special treatment that λ deserves, the field-dependent rate-constants have been computed as the combination of the field-free rate constant, $k_{CT}(0)$, where the λ_{ext} has been taken into account,[51] and a correction for the presence of the field by the addition of the field-dependent quantity $k_{CT}(\mathbf{F}) - k_{CT}(0)$, computed setting $\lambda_{ext} = 0$ for both rates, the $k_{CT}(\mathbf{F})$ and $k_{CT}(0)$. The final derived $k_{CT}(\mathbf{F})$ is given by $k_{CT}(\mathbf{F}) = k_{CT}(0, \lambda = \lambda_{int} + \lambda_{ext}) + k_{CT}(\mathbf{F}, \lambda = \lambda_{int}) - k_{CT}(0, \lambda = \lambda_{int})$.

Theoretical background

Owing to the zwitterionic nature of the CTSs, such states are expected to have considerably larger dipole moments than the ground state or the LES. In other words, the change of the dipole moment in the CT reaction is large, and it dominates the Taylor expansion (2). Consequently, for the CT reaction, Eq. (2) can be safely truncated down to the following equation:

$$\Delta G_{CT}(\mathbf{F}) = \Delta G_{CT}(0) - \Delta\mu_{CT}\mathbf{F}. \tag{8}$$

Yet, for **ZnTTP**, we have tested the accuracy of Eq. (8) to compute the difference between the field-dependent energies of CTS_1 and LES_1 with respect to the field-dependent energies obtained with Eq. (2), including the second term correction, i.e., the polarizability changes. To our delight, the maximum difference including or not including the second-order corrections was less than 0.02 eV for the range of electric fields studied (for details, see Table S1 in the supplementary material). Therefore, we concluded that Eq. (8) can be safely used as it retains a proper description of the field-dependent difference in energy between the states of interest.

To impose the desired constraint [i.e., $\Delta G(\mathbf{F}) = -\lambda(\mathbf{F})$], one should determine the strength and orientation of **F** for which the value of $\Delta G(\mathbf{F})$ given by Eq. (8) is equal to the value of $-\lambda(\mathbf{F})$ provided by an homologous Taylor expansion for $-\lambda$ [i.e., $-\lambda(\mathbf{F}) = -\lambda_0 - (\partial\lambda/\partial F)\cdot\mathbf{F}\ldots$). Nevertheless, it turns out that the change of $-\lambda$ due to the OEEF is negligible compared to the change of the Gibbs energy in the $LES_1 \rightarrow CTS_1$ transition in the presence of an OEEF, and therefore the approximation $-\lambda(\mathbf{F}) = -\lambda_0 - (\partial\lambda/\partial F)\cdot\mathbf{F} \approx -\lambda_0$ can be safely used (see Fig. 2). Therefore, the final working equation to obtain the optimal field-strength (**OFS**) that maximizes k_{CT} is (see derivation in the supplementary material),

$$\mathbf{OFS} = \frac{\Delta G(0) + \lambda}{\Delta\mu}. \tag{9}$$

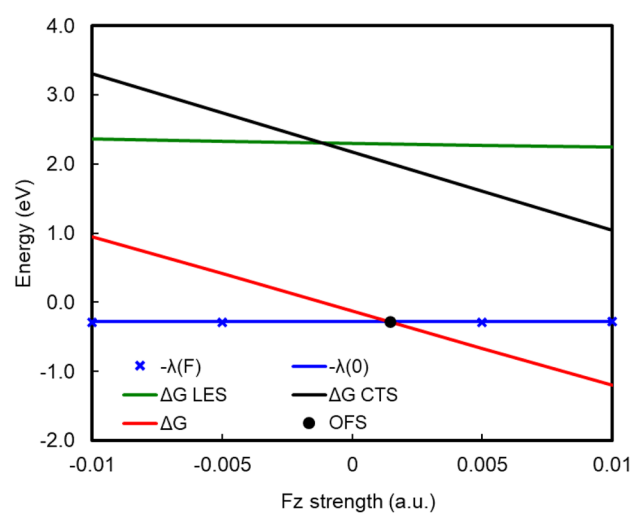

FIG. 2. Field-dependent LES_1 to CTS_1 ΔG (red), $-\lambda(0)$ (blue), $-\lambda(\mathbf{F})$ (blue crosses), and determination of **OFS** (crossing point, black) for **ZnTTP**. LES_1 (green) and CTS_1 (black) ΔG energies are given with respect to the ground-state Gibbs energy.

The optimal direction in the space of the **OFS** is given by the difference between the dipole moments of the CT excited state and the LES_1 state, $\Delta\mu$. In this work, we have aligned the Z axis with the $\Delta\mu$ vector (see Fig. 1), which generally coincides with the axis generated by the region of the space where the electrons and holes are created during the CT process.

The difference between the **OFS** predicted with Eq. (9) and the corresponding equation, including the dependence of λ with the OEEF strength for **ZnTTP**, is lower than the resolution of possible experimental setups (i.e., <1 mV/Å). The same assumption holds for the other systems studied in this work, with a maximum difference of 1.2 mV/Å (see Table S2 in the supplementary material for further details). We will refer to the new methodology to compute **OFS** and determine k_{CT}'s as Field-Dependent-Barrier for Charge-Transfer (FDB-CT) reactions.

Figure 2 summarizes the field-induced changes on Gibbs excitation energies for CTS_1 and LES_1 [$\Delta G_{CTS1}(\mathbf{F})$, $\Delta G_{LES1}(\mathbf{F})$]; for the transition between these two states, $\Delta G_{CT}(\mathbf{F})$; the negative of field-dependent reorganization energy, $-\lambda_{LES1\rightarrow CTS1}(\mathbf{F})$; and the **OFS**. For convenience, hereafter, $\Delta G_{CT}(\mathbf{F})$ and $-\lambda_{LES1\rightarrow CTS1}(\mathbf{F})$ are referred to as ΔG and −λ, respectively. The distance between the blue and red lines of Fig. 2 determines the value of the term (ΔG − λ) in Eq. (1) as a function of the **F** strength.

To test the validity of the FDB-CT approach, we have computed for **ZnTTP** the variation of ΔG, λ, $(\lambda + \Delta G)^2$, and k_{CT} in the presence of explicit OEEFs judiciously oriented such that the positive and negative poles lie in the direction where the electron and the hole of the CTS are located at **F** = 0, respectively. For this test, the **ZnTTP** optimal geometry in the presence of the EF was used. The strength of such OEEFs was selected to be $\mathbf{F_1}$ = 0, and $\mathbf{F_2}$ = 1.45 × 10^{-3} a.u. (74.7 mV/Å); being $\mathbf{F_2}$ the **OFS** of **ZnTTP** computed with Eq. (9). The largest k_{CT} predicted by the FDB-CT method is the one given by the **OFS** (3.34 × 10^{11} s^{-1}). k_{CT}(**OFS**) is almost twice as large as the field free $k_{CT}(0)$ (1.8 × 10^{11} s^{-1}) and corresponds to the theoretical limit of the k_{CT} for this system. Calculations using explicit electric fields (i.e., without any approximation) at $\mathbf{F_2}$ field-strength give a smaller value for $(\lambda + \Delta G)^2$ than the one at **F** = 0, which then leads to a larger k_{CT} (3.31 × 10^{11} s^{-1}). To our delight, the rate constants computed considering explicit external electric fields are very similar to the predictions obtained with the FDB-CT method. The origin of the small differences is (i) the first-order truncation used in the application of Eq. (2); (ii) the field-dependence of λ and the

TABLE I. Predicted and experimental charge-transfer rate parameters for **ZnTTP**, **TPA**, **Az**, and **PC** computed through the FDB-CT method or under explicit judiciously selected OEEFs.[a] Experimental values are always measured at F = 0.[b]

OEEF (a.u.)	ΔG (eV)	λ_{int} (eV)	$(\lambda + \Delta G)^2$ (eV^2)	k_{CT} (s^{-1})
ZnTTP				
Experimental[21]				2.9×10^{10}
0.00	−0.125	0.281	0.057	1.11×10^{10}
1.45×10^{-3} (OFS)	−0.281	0.281	0.0	1.87×10^{11}
1.45×10^{-3} (OFS)	−0.260[c]	0.264[c]	1.6×10^{-5}[c]	1.83×10^{11}[c]
Point charge (1.29×10^{-3})	−0.281	0.204	5.9×10^{-3}	1.51×10^{11}
TPA				
Experimental[23]				6×10^{10}
0.00	−0.96	0.210	0.563	2.46×10^{10}
-1.54×10^{-3} (OFS)	−0.210	0.210	0.000	1.03×10^{11}
Az				
Experimental[24]				2×10^{10}
0.00	0.20	0.240	0.194	3.29×10^{9}
1.58×10^{-3} (OFS)	−0.24	0.240	0.000	1.45×10^{14}
PC				
Experimental[25]				1.25×10^{12}
0.00	−0.178	0.134	0.078	3.75×10^{13}
-3.47×10^{-4} (OFS_1)	−0.134	0.134	0.000	5.79×10^{13}
-8.9×10^{-3} (OFS_2)	−0.366	0.366	0.000	2.98×10^{11}

[a]Electronic couplings for **ZnTPP**, **TPA**, **Az**, and **PC** are 0.0031, 0.0015, 0.0735, and 0.0525 eV, respectively.
[b]Root-mean square errors in vertical excitation energies calculated with popular density functionals vary from ~0.3 to 0.7 eV, with range corrected functionals such as CAM-B3LYP being among the most accurate.[70] These errors translate into similar errors for ΔG and, consequently, differences between experimental and computed k_{CT} of one order of magnitude or even larger are commonly found.[51]
[c]Values computed using explicit OEEF.

coupling term, which in the FDB-CT are considered constant and equal to the field-free value; and (iii) the minor changes in equilibrium geometry induced by the external electric field.

Deviations of FDB-CT may also be expected when a very intense field is applied (i.e., $F \geq 10^{-2}$ a.u.; see Table S4 in the supplementary material), as it can trigger perturbations and transformations of the excited states that are beyond the scope of prediction of our computational model. Despite the FDB-CT approximations, considering that FDB-CT has a far lower computational cost than the calculations performed with explicit OEEF, it becomes a low-cost and efficient tool to explore the dependence of k_{CT} with respect to different OEFFs and to determine the **OFS** for a given D–A dyad.

RESULTS AND DISCUSSION

Once the performance of our computational model was validated for **ZnTTP**, we used the FDB-CT method to determine the **OFS** for three more dyads, namely **TPA**, **Az**, and **PC**. For **TPA**, the predicted field-free rate constant is $k_{CT} = 2.46 \times 10^{10}$ s^{-1}. FDB-CT predicts for this system an **OFS** equal to -1.54×10^{-3} a.u. (−79.2 mV/Å), and the rate constant under the presence of such an OEEF is predicted to increase 4-fold to $k_{CT} = 1.03 \times 10^{11}$ s^{-1} (see Fig. S2 in the supplementary material).

Regarding the **Az** system, without an electric field, the rate constant k_{CT} is 3.29×10^{9} s^{-1}.[51] However, by applying the **OFS** (1.58×10^{-3} a.u.), the k_{CT} is boosted to 1.45×10^{14} s^{-1} (see Fig. S3 in the supplementary material). Such a sharp enlargement of the rate constant corresponds to a 4400-fold increase and is the highest reported in this manuscript. Although the Marcus equation is less accurate for the prediction of k_{CT} values in very fast CT processes, the **OFS** predicted by our method will be quite similar to the electric field that maximizes the actual value of k_{CT}.

The enhancement in the CT rate for **Az** can be explained by the change in the thermodynamics of the process induced by the electric field. Specifically, **Az** is the only system that presents an unfavorable CT ($\Delta G = 0.20$ eV, see Table I), while λ and $\Delta\mu$ are similar to the rest of the systems. The **OFS** transforms the process from endergonic to exergonic ($\Delta G = -0.24$ eV) by stabilizing the charge-transfer state, thus largely facilitating the CT and then increasing its CT rate constant.

The high boost reported for **Az** clearly demonstrates that although using OEEFs to enhance the rate constant is always a valid strategy, for some particular D–A dyads, it has a greater impact due to their intrinsic chemical nature. Specifically, the room for improvement in terms of k_{CT} enhancement for a particular D–A dyad is directly proportional to its $(\Delta G - \lambda_{tot})^2$ value at F = 0, and whether such improvement is reached at reasonable fields depends on the $\Delta\mu_{CT}$. FDB-CT can be used to find the D–A dyads for which k_{CT} has a stronger dependence on the OEEF.

However, it should be mentioned that in particular scenarios where there are several low-lying LESs below the CTS, the chances of state recombinations or other situations that are not accounted for by the FDB-CT method increase, and therefore it may lead to a divergence between the k_{CT} predicted by FDB-CT and the experimental observations or the use of explicit OEEFs.

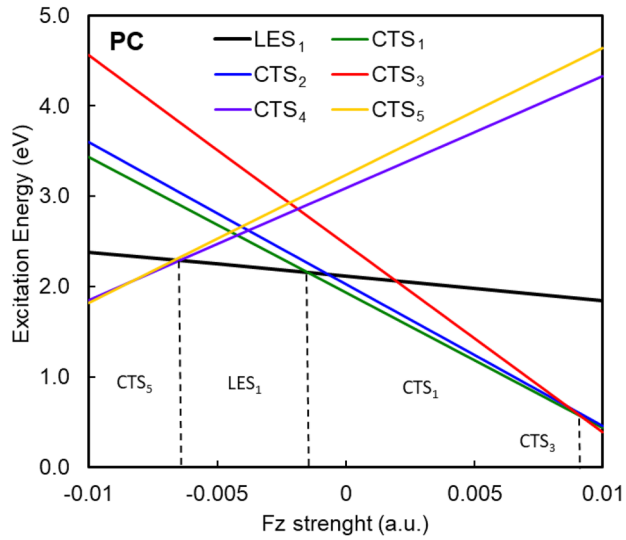

FIG. 3. Field-dependent excitation energy for the relevant excited states in **PC**: LES_1, CTS_1, CTS_2, CTS_3, CTS_4, and CTS_5.

In the case of the **PC** system, we have determined that there exist several excited states that correspond to an electron transfer from the phthalocyanine group (Pht) to the $C_{59}N$, as for instance, CTS_1 [charge separation (CS) = 0.870 e], CTS_2 (CS = 0.853 e), and CTS_3 (CS = 0.926 e); while some other excited states are better described as the electron transfer from the $C_{59}N$ to the Pht unit in **PC**, as it turns out to be the case for CTS_4 (CS = 0.738 e) or CTS_5 (CS = 0.822 e) (see the supplementary material for further details). Since the sign of the electric field represents its orientation in space, this distinct behavior is very easily recognized by looking at the sign of the slopes that such states present in Fig. 3. It is worth remarking that the slopes are given by the change of the dipole moment in the charge transfer process from LES_1 to CTS_n and, therefore, are directly proportional to the charge-separation parameter, CS [$CS^i = \Omega^i(D, A) - \Omega^i(A, D)$].

A given state can be stabilized at will by fine-tuning the direction and strength of the OEEF. In the particular case of **PC** (Fig. 3), by placing an OEEF with the positive pole on the $C_{59}N$ side (we have adopted an F > 0 convention) and the negative pole on the Pht side, one can obtain the most stable excited state, the CTS_1 when $F < 8 \times 10^{-3}$ a.u. and the CTS_3 when $F > 8 \times 10^{-3}$ a.u.

On the other hand, by switching the direction of the OEEF (F < 0), one obtains the most stable excited state CTS_5 for $|F| > 6.7 \times 10^{-3}$ a.u., while for $6.7 \times 10^{-3} > |F| > 1.5 \times 10^{-3}$ a.u., the most stable excited state becomes LES_1 (thus, in this range of fields, the CT reaction is endergonic). Finally, for $|F| < 1.5 \times 10^{-3}$ a.u., CTS_1 is the most stable state. Note that at F = 0, CTS_1 is the first excited state.

Having this in mind, we have determined two different **OFSs**, namely $\mathbf{OFS_1}$ and $\mathbf{OFS_2}$, which will correspond to the **OFS** for the Pht-to-$C_{59}N$ ($LES_1 \rightarrow CTS_1$) and the $C_{59}N$-to-Pht ($LES_1 \rightarrow CTS_2$) electron transfers, respectively (Fig. 4). The field-free k_{CT} is 3.75×10^{13} s^{-1} for the Pht-to-$C_{59}N$ charge transfer. The predicted OFS_1 is located at -3.47×10^{-4} a.u. (17.8 mV/Å), and its corresponding predicted k_{CT} is 5.79×10^{13} s^{-1}, which represents a slight increase

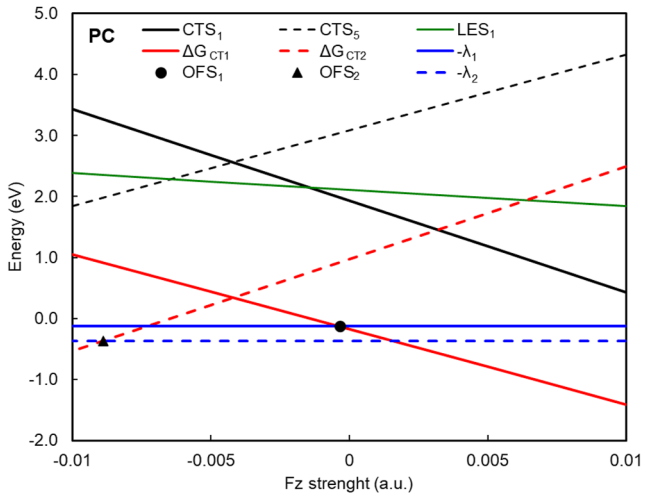

FIG. 4. Energy dependence of ΔG in **PC**: solid for CTS_1 and dashed for CTS_5; −λ (blue), and determination of OFS_1 (black dot) and OFS_2 (black triangle). The LES_1, CTS_1, and CTS_5 energies are given with respect to the ground-state energy.

with respect to the F = 0 scenario. For the reverse charge transfer, the **OFS_2** is -8.9×10^{-3} a.u. (−457.7 mV/Å), and the charge-transfer rate is 2.2×10^{11} s^{-1}. However, the charge transfer occurring at OFS_2 is purely a field-induced process since it was non-existent at field-free, as CTS_4 is more than 1 eV higher in energy than the other lower-lying CTSs. Taking into account the large magnitude of **OFS_2**, the reliability of the FDB-CT prediction for this particular OEEF is lower than for the other values presented in this paper.

To finalize, we have examined the effect on the charge-transfer rate constant of two opposite point-charge models, located at ±20.8 Å from the D–A junction of **ZnTTP**, which generate a non-homogeneous electric field of analogous strength and direction to the **OFS** predicted by Eq. (8). The calculated ΔG = −0.281 eV matches the values predicted using the FDB-CT approach for the **OFS** (with the number of figures reported), and it is in very good agreement with the value of −0.260 eV predicted by explicit OEEFs; analogously, the obtained rate constant of $k_{CT} = 2.98 \times 10^{11}$ s^{-1} is very close to the 3.31×10^{11} s^{-1} (3.34×10^{11} s^{-1}) value obtained with an explicit homogeneous electric field (FDB-CT method). Such results open the door for using FDB-CT to simulate the effect of charged functional groups on the k_{CT}, which could be one of the keys to improving the rational design of highly efficient DSSCs based on D–A dyads.

CONCLUSIONS

We have proposed a simple analytical approach to compute in a straightforward manner the field-dependent excitation energies for any D–A dyad (it can also be applied to D–A–D triads, etc.). With a very simple linear formula, our computational approach determines the optimal direction and strength of the OEEF needed to maximize the charge-transfer rate in the framework of Marcus theory. FDB-CT predicts the field-induced changes of the energy of any excited state, and therefore all possible combinations of LES to CTS transitions can be studied separately. To validate the FDB-CT method, we have performed charge-transfer rate calculations in the presence of explicit electric fields, obtaining **OFS** results matching those obtained with the FDB-CT approach. We have analyzed several fullerene-based molecular dyads and, for each of them, determined the optimal electric field that maximizes its charge-transfer rate constant, normally by stabilizing the charge-transfer states. For all the systems studied, **OFS** has yielded a larger k_{CT} than the one obtained at F = 0. The potential enhancement of k_{CT} depends on the value of $(\Delta G + \lambda_{tot})^2$ for each particular system calculated at F = 0, while $\Delta\mu_{CT}$ controls whether such enhancement is feasible to be obtained at reasonable small fields. The highest k_{CT} enhancement predicted in this work is about 4400-fold with respect to the field-free value. Furthermore, visual inspection of the figures representing the results obtained from Eq. (8) gives insight into (i) the predicted changes induced by the OEEF in the energy of the relevant states; (ii) the order and nature (LES/CTS) of excited states as a function of the electric field applied; and (iii) the possibility of controlling the movement of the electron and hole participating in the charge transfer process.

There are two clear limitations in our approach: (i) the calculation of k_{CT} with the Marcus approach in the case of very fast charge transfer processes is unreliable, and (ii) the reliability of the FDB-CT predictions decreases when the strength of the electric field is very high because of the truncation error in Eq. (2) due to the first-order approximation used. Despite these limitations, we think that our FDB-CT approach can assist in the rational design of D–A dyads with large k_{CT} induced by an OEEF or by a local field generated by charged or polar functional groups.

SUPPLEMENTARY MATERIAL

Full derivation and justification of Eq. (9), ΔG(**F**) and Δλ(**F**) for all the systems, analysis of the **$C_{59}N$** excited states, graphical representation of Eq. (8) for **TPA** and **Az** systems, and Cartesian coordinates.

ACKNOWLEDGMENTS

This work was supported with funds from the Spanish Ministerio de Ciencia e Innovación (Project Nos. PID2020-13711GB-I00 and PGC2018-098212-B-C22) and the Generalitat de Catalunya (Project No. 2021SGR623). We acknowledge the Spanish government for the predoctoral grant to P.B.-S. (Grant No. FPU17/02058). We are also grateful for the computational time financed by the Consorci de Serveis Universitaris de Catalunya (CSUC).

AUTHOR DECLARATIONS

Conflict of Interest

The authors have no conflicts to disclose.

Author Contributions

P.B.-S. and A.A.V. performed all the calculations. P.B.-S. analyzed the results and wrote the first draft of the manuscript. A.A.V., J.M.L., and M.S. devised and supervised the project. The manuscript

was written with the contributions of all authors. All authors have given approval to the final version of the manuscript.

Pau Besalú-Sala: Formal analysis (lead); Investigation (lead); Methodology (lead); Writing – original draft (equal); Writing – review & editing (equal). **Alexander A. Voityuk**: Formal analysis (equal); Investigation (supporting); Methodology (lead); Writing – review & editing (equal). **Josep M. Luis**: Conceptualization (equal); Funding acquisition (equal); Supervision (equal); Writing – review & editing (equal). **Miquel Solà**: Conceptualization (equal); Funding acquisition (lead); Supervision (equal); Writing – original draft (equal); Writing – review & editing (equal).

DATA AVAILABILITY

The data that support the findings of this study are available within the article and its supplementary material.

REFERENCES

[1] E. Sjulstok, J. M. H. Olsen, and I. A. Solov'yov, Sci. Rep. **5**, 18446 (2015).
[2] C. Léger and P. Bertrand, Chem. Rev. **108**, 2379 (2008).
[3] V. Vaissier Welborn and T. Head-Gordon, Chem. Rev. **119**, 6613 (2019).
[4] *Proton-Coupled Electron Transfer: A Carrefour of Chemical Reactivity Traditions*, *Catalysis Series Vol. 157*, edited by S. Formosinho and M. Barroso (The Royal Society of Chemistry, Cambridge, 2011).
[5] *Fundamental Neuroscience*, 4th ed., edited by L. R. Squire, D. Berg, F. E. Bloom, S. du Lac, A. Ghosh, and N. C. Spitzer (Academic Press, San Diego, 2013).
[6] J. Withmarsh and Govindjee, in *Concepts in Photobiology: Photosynthesis and Photomorphogenesis*, edited by G. S. Singhal *et al.* (Narosa Publishing House, New Delhi, 1999), p. 11.
[7] N. G. Smith and J. S. Dukes, Global Change Biol. **19**, 45 (2013).
[8] S. Weber, Biochim. Biophys. Acta, Bioenerg. **1707**, 1 (2005).
[9] R. A. Marcus, J. Chem. Phys. **24**, 966 (1956).
[10] C. Zhu, H. Yue, B. Maity, I. Atodiresei, L. Cavallo, and M. Rueping, Nat. Catal. **2**, 678 (2019).
[11] B. Maity, C. Zhu, H. Yue, L. Huang, M. Harb, Y. Minenkov, M. Rueping, and L. Cavallo, J. Am. Chem. Soc. **142**, 16942 (2020).
[12] Transforming Our World: The 2030 Agenda for Sustainable Development (A/RES/70/1), UN General Assembly, New York, 2015.
[13] D. Jariwala, V. K. Sangwan, L. J. Lauhon, T. J. Marks, and M. C. Hersam, Chem. Soc. Rev. **42**, 2824 (2013).
[14] Y. He and Y. Li, Phys. Chem. Chem. Phys. **13**, 1970 (2011).
[15] A. Zieleniewska, F. Lodermeyer, A. Roth, and D. M. Guldi, Chem. Soc. Rev. **47**, 702 (2018).
[16] J. L. Segura, N. Martín, and D. M. Guldi, Chem. Soc. Rev. **34**, 31 (2005).
[17] S. M. Pratik and A. Datta, Phys. Chem. Chem. Phys. **15**, 18471 (2013).
[18] G. Gryn'ova, J. M. Barakat, J. P. Blinco, S. E. Bottle, and M. L. Coote, Chem. - Eur. J. **18**, 7582 (2012).
[19] R. Kacimi, M. Bourass, T. Toupance, N. Wazzan, M. Chemek, A. El Alamy, L. Bejjit, K. Alimi, and M. Bouachrine, Res. Chem. Intermed. **46**, 3247 (2020).
[20] K. Galappaththi, P. Ekanayake, and M. I. Petra, Sol. Energy **161**, 83 (2018).
[21] D. M. Guldi, C. Luo, M. Prato, E. Dietel, and A. Hirsch, Chem. Commun. **2000**, 373.
[22] J. P. Martínez, S. Osuna, M. Solà, and A. Voityuk, Theor. Chem. Acc. **134**, 12 (2015).
[23] J. P. Martínez, M. Solà, and A. A. Voityuk, J. Comput. Chem. **37**, 1396 (2016).
[24] T. Makinoshima, M. Fujitsuka, M. Sasaki, Y. Araki, O. Ito, S. Ito, and N. Morita, J. Phys. Chem. A **108**, 368 (2004).
[25] G. Rotas, J. Ranta, A. Efimov, M. Niemi, H. Lemmetyinen, N. Tkachenko, and N. Tagmatarchis, ChemPhysChem **13**, 1246 (2012).
[26] R. A. Marcus, Rev. Mod. Phys. **65**, 599 (1993).
[27] K. M. Pelzer and S. B. Darling, Mol. Syst. Des. Eng. **1**, 10 (2016).
[28] P. F. Barbara, T. J. Meyer, and M. A. Ratner, J. Phys. Chem. **100**, 13148 (1996).
[29] D. Wróbel and A. Graja, Coord. Chem. Rev. **255**, 2555 (2011).
[30] F. D'Souza, R. Chitta, K. Ohkubo, M. Tasior, N. K. Subbaiyan, M. E. Zandler, M. K. Rogacki, D. T. Gryko, and S. Fukuzumi, J. Am. Chem. Soc. **130**, 14263 (2008).
[31] M. Izquierdo, B. Platzer, A. J. Stasyuk, O. A. Stasyuk, A. A. Voityuk, S. Cuesta, M. Solà, D. M. Guldi, and N. Martín, Angew. Chem., Int. Ed. **58**, 6932 (2019).
[32] S. Zank, J. M. Fernández-García, A. J. Stasyuk, A. A. Voityuk, M. Krug, M. Solà, D. M. Guldi, and N. Martín, Angew. Chem., Int. Ed. **61**, e202112834 (2022).
[33] Y. Guo, W. Shi, and Y. Zhu, EcoMat **1**, e12007 (2019).
[34] R. A. Marsh, J. M. Hodgkiss, and R. H. Friend, Adv. Mater. **22**, 3672 (2010).
[35] X. Wang, H. Wang, M. Zhang, T. Pullerits, and P. Song, J. Phys. Chem. C **127**, 2805 (2023).
[36] S. Zhu, D. Kang, Z. Liu, M. Zhang, Y. Ding, and P. Song, J. Phys. Chem. A **126**, 3669 (2022).
[37] S. Shaik, D. Danovich, J. Joy, Z. Wang, and T. Stuyver, J. Am. Chem. Soc. **142**, 12551 (2020).
[38] T. Stuyver, D. Danovich, J. Joy, and S. Shaik, Wiley Interdiscip. Rev.: Comput. Mol. Sci. **10**, e1438 (2020).
[39] S. Shaik, R. Ramanan, D. Danovich, and D. Mandal, Chem. Soc. Rev. **47**, 5125 (2018).
[40] D. J. Hanaway and C. R. Kennedy, J. Org. Chem. **88**, 106 (2023).
[41] J. M. Bofill, W. Quapp, G. Albareda, I. d. P. R. Moreira, and J. Ribas-Ariño, J. Chem. Theory Comput. **18**, 935 (2022).
[42] J. M. Bofill, W. Quapp, G. Albareda, I. d. P. R. Moreira, J. Ribas-Ariño, and M. Severi, Theor. Chem. Acc. **142**, 22 (2023).
[43] S. Yu, P. Vermeeren, T. A. Hamlin, and F. M. Bickelhaupt, Chem. - Eur. J. **27**, 5683 (2021).
[44] S. P. de Visser, G. Mukherjee, H. S. Ali, and C. V. Sastri, Acc. Chem. Res. **55**, 65 (2022).
[45] P. Besalú-Sala, M. Solà, J. M. Luis, and M. Torrent-Sucarrat, ACS Catal. **11**, 14467 (2021).
[46] A. D. Becke, J. Chem. Phys. **98**, 5648 (1993).
[47] C. Lee, W. Yang, and R. G. Parr, Phys. Rev. B **37**, 785 (1988).
[48] R. Krishnan, J. S. Binkley, R. Seeger, and J. A. Pople, J. Chem. Phys. **72**, 650 (1980).
[49] S. Grimme, J. Antony, S. Ehrlich, and H. Krieg, J. Chem. Phys. **132**, 154104 (2010).
[50] S. Grimme, S. Ehrlich, and L. Goerigk, J. Comput. Chem. **32**, 1456 (2011).
[51] P. Besalú-Sala, A. A. Voityuk, J. M. Luis, and M. Solà, Phys. Chem. Chem. Phys. **23**, 5376 (2021).
[52] M. Dierksen and S. Grimme, J. Phys. Chem. A **108**, 10225 (2004).
[53] M. J. G. Peach, P. Benfield, T. Helgaker, and D. J. Tozer, J. Chem. Phys. **128**, 044118 (2008).
[54] M. R. Silva-Junior, M. Schreiber, S. P. A. Sauer, and W. Thiel, J. Chem. Phys. **129**, 104103 (2008).
[55] M. Isegawa, R. Peverati, and D. G. Truhlar, J. Chem. Phys. **137**, 244104 (2012).
[56] A. D. Laurent and D. Jacquemin, Int. J. Quantum Chem. **113**, 2019 (2013).
[57] C. Suellen, R. G. Freitas, P.-F. Loos, and D. Jacquemin, J. Chem. Theory Comput. **15**, 4581 (2019).
[58] R. Grotjahn and M. Kaupp, J. Chem. Theory Comput. **16**, 5821 (2020).
[59] F. Weigend and R. Ahlrichs, Phys. Chem. Chem. Phys. **7**, 3297 (2005).
[60] A. J. Stasyuk, O. A. Stasyuk, M. Solà, and A. A. Voityuk, J. Phys. Chem. B **124**, 9095 (2020).
[61] A. J. Stasyuk, O. A. Stasyuk, M. Solà, and A. A. Voityuk, Dalton Trans. **50**, 16214 (2021).
[62] A. J. Stasyuk, O. A. Stasyuk, M. Solà, and A. A. Voityuk, J. Mater. Chem. C **9**, 9436 (2021).
[63] O. A. Stasyuk, A. J. Stasyuk, M. Solà, and A. A. Voityuk, Nanoscale Adv. **4**, 2180 (2022).

[64] A. J. Stasyuk, O. A. Stasyuk, M. Solà, and A. A. Voityuk, Chem. - Eur. J. **26**, 10896 (2020).
[65] T. Yanai, D. P. Tew, and N. C. Handy, Chem. Phys. Lett. **393**, 51 (2004).
[66] M. J. Frisch, G. W. Trucks, H. B. Schlegel, G. E. Scuseria, M. A. Robb, J. R. Cheeseman, G. Scalmani, V. Barone, G. A. Petersson, H. Nakatsuji, X. Li, M. Caricato, A. V. Marenich, J. Bloino, B. G. Janesko, R. Gomperts, B. Mennucci, H. P. Hratchian, J. V. Ortiz, A. F. Izmaylov, J. L. Sonnenberg, D. Williams-Young, F. Ding, F. Lipparini, F. Egidi, J. Goings, B. Peng, A. Petrone, T. Henderson, D. Ranasinghe, V. G. Zakrzewski, J. Gao, N. Rega, G. Zheng, W. Liang, M. Hada, M. Ehara, K. Toyota, R. Fukuda, J. Hasegawa, M. Ishida, T. Nakajima, Y. Honda, O. Kitao, H. Nakai, T. Vreven, K. Throssell, J. A. Montgomery, Jr., J. E. Peralta, F. Ogliaro, M. J. Bearpark, J. J. Heyd, E. N. Brothers, K. N. Kudin, V. N. Staroverov, T. A. Keith, R. Kobayashi, J. Normand, K. Raghavachari, A. P. Rendell, J. C. Burant, S. S. Iyengar, J. Tomasi, M. Cossi, J. M. Millam, M. Klene, C. Adamo, R. Cammi, J. W. Ochterski, R. L. Martin, K. Morokuma, O. Farkas, J. B. Foresman, and D. J. Fox, Gaussian 16, Revision B.01, Wallingford, CT, 2016.
[67] A. V. Luzanov and O. A. Zhikol, Int. J. Quantum Chem. **110**, 902 (2010).
[68] F. Plasser and H. Lischka, J. Chem. Theory Comput. **8**, 2777 (2012).
[69] A. A. Voityuk, J. Phys. Chem. C **117**, 2670 (2013).
[70] J. Liang, X. Feng, D. Hait, and M. Head-Gordon, J. Chem. Theory Comput. **18**, 3460 (2022).